# Characterization of ICAM-2 and Evidence for a Third Counter-Receptor for LFA-1

By Antonin R. de Fougerolles,* Steven A. Stacker,* Roland Schwarting,‡ and Timothy A. Springer*

*From the *Committee on Immunology, Department of Pathology, Harvard Medical School, and Center for Blood Research, Boston, Massachusetts 02115; and the ‡Department of Pathology, Thomas Jefferson University, Philadelphia, Pennsylvania 19107*

## Summary

In an endeavor to further characterize human intercellular adhesion molecule-2 (ICAM-2), two murine monoclonal antibodies (mAb) were generated to ICAM-2 transfected COS cells, and designated CBR-IC2/1 and CBR-IC2/2. Immunoprecipitated, reduced ICAM-2 migrated as a broad band of $M_r$ 60,000 in sodium dodecyl sulfate-polyacrylamide gel electrophoresis. Treatment with N-glycanase revealed a peptide backbone of $M_r$ 31,000, consistent with the size predicted from the cDNA. ICAM-2 had a broad distribution on hematopoietic cell lines and little expression on other cell lines, the sole exception being cultured endothelial cells which possess high levels of ICAM-2. Resting lymphocytes and monocytes expressed ICAM-2, while neutrophils did not. Staining of tissue sections with anti–ICAM-2 mAb confirmed their strong reactivity to vascular endothelium, but demonstrated a lack of ICAM-2 expression on other tissues. Small clusters of ICAM-2 positive cells were, however, seen in germinal centers. In contrast to ICAM-1 there was little or no induction of ICAM-2 expression on lymphocytes or cultured endothelium upon stimulation with inflammatory mediators. One of the two mAb, CBR-IC2/2, was found to totally inhibit binding of ICAM-2$^+$ COS cells to purified lymphocyte function–associated antigen-1 (LFA-1). Using this mAb, LFA-1–dependent binding to both stimulated and unstimulated endothelium was found to be totally accounted for by ICAM-1 and ICAM-2. Homotypic aggregation of an Epstein-Barr virus-transformed B cell line, JY, was found to be solely ICAM-1 and ICAM-2–dependent, while in the case of the T cell lymphoma cell line, SKW3, anti- ICAM-2 mAb in conjunction with anti–ICAM-1 mAb could not inhibit the LFA-1–dependent aggregation. This suggests an additional LFA-1 ligand exists. Using a cell binding assay to purified LFA-1 in conjunction with anti–ICAM-1 and anti–ICAM-2 mAb, we have demonstrated that this putative third ligand for LFA-1 exists on SKW3 and other cell lines.

Adhesion molecules play a central role in the functions of the immune system. These molecules direct cell-cell interactions critical for antigen presentation, lymphocyte activation, localization, migration, and effector/target functions at the site of inflammation (reviewed in reference 1). The integrin family of adhesion receptors are involved in the cell-cell and cell-matrix interactions of a wide variety of cell types (1–4). A subgroup of the integrins, consisting of lymphocyte function–associated antigen-1 (LFA-1),[1] Mac-1, and p150,95 (the "leukocyte integrins") play a major role in leukocyte adhesion (5). They share a common $\beta$ subunit (CD18) noncovalently associated with homologous $\alpha$ subunits (LFA-1 $\alpha$, CD11a; Mac1 $\alpha$, CD11b; p150,95 $\alpha$, CD11c) (6). Their importance in leukocyte adhesion is most aptly demonstrated by a clinical condition, known as leukocyte adhesion deficiency (7). Patients have recurrent life-threatening bacterial infections due to mutations in the common $\beta$ subunit, resulting in lack of expression of all three leukocyte integrins (8).

Of the three leukocyte integrins, LFA-1 has the best characterized role in cell adhesion. It was first defined by the ability of mAb to block both T cell-mediated killing and proliferation, and is required for numerous other functions including T helper and B lymphocyte responses, natural killing, Ab-dependent cellular cytotoxicity by monocytes and granulocytes, and adherence of leukocytes to endothelial cells, fibroblasts, and epithelial cells (5, 9). An inducible molecule, intercellular adhesion molecule-1 (ICAM-1) (CD54), was the first ligand discovered for LFA-1 (10, 11). A member of the immunoglobulin superfamily (12, 13), ICAM-1 has five Ig-like

[1] *Abbreviations used in this paper:* AP, alkaline phosphatase; FDC, follicular dendritic cells; HUVEC, human umbilical vein endothelial cells; ICAM, intercellular adhesion molecule; LFA, lymphocyte function–associated antigen.


J. Exp. Med. © The Rockefeller University Press • 0022-1007/91/07/0253/15 $2.00
Volume 174 July 1991 253–267

domains with the binding site for LFA-1 localized to specific residues in the first N-terminal domain (14). Most LFA-1–dependent phenomena could be inhibited by blocking mAb to ICAM-1 (10, 15, 16). However, binding of lymphocytes to cultured human umbilical vein endothelial cells (HUVEC) showed that the ICAM-1 blocking mAb, RR1/1, could not inhibit all the LFA-1–dependent adhesion (15). This implied a second ligand for LFA-1 existed on endothelial cells. Similarly, LFA-1 mAb but not ICAM-1 mAb blocked PMA-induced aggregation of a T cell lymphoblastoid cell line, SKW3 (10). Lastly, LFA-1–dependent cytolysis of certain target cells by T cells was not inhibitable with mAb to ICAM-1 (16), further evidence for additional LFA-1 ligands. A cDNA clone for a second LFA-1 ligand, termed ICAM-2, was obtained by transfecting COS cells with an endothelial cDNA library and selecting for binding to LFA-1 coated plates in the presence of blocking ICAM-1 mAb (17). Like ICAM-1, ICAM-2 is a member of the immunoglobulin superfamily. It has only two immunoglobulin-like domains that are most homologous to the two N-terminal domains of ICAM-1, with 35% amino acid identity (17).

In this study we report on the biochemical and cellular nature of ICAM-2 using mAb generated to COS cells transiently expressing the ICAM-2 cDNA. Two murine mAb to ICAM-2, CBR-IC2/1 and CBR-IC2/2, were generated. Using these antibodies, the cellular and tissue distribution, biochemical properties and functional role in cell-cell adhesion of ICAM-2 could be studied. ICAM-2 was found to differ from ICAM-1 in both its distribution and inducibility, implying a functional difference between the two molecules. Several LFA-1–dependent, ICAM-1–independent cell interactions could be accounted for by ICAM-2, whereas others revealed the presence of a third, as yet undefined, ligand for LFA-1.

## Materials and Methods

*Monoclonal Antibodies.* The following previously described murine mAbs to human antigens were used: TS2/9 (anti-LFA-3, IgG1) (18), TS2/16 (anti-CD29, IgG1) (18), TS1/22 (anti-CD11a, IgG1) (18), RR1/1 (anti-ICAM-1, IgG1) (10), W6/32 (anti-HLA-A,B,C, IgG2a) (19), and X63 (nonbinding antibody, IgG1).

*Cell Culture.* The murine myeloma P3X63Ag8.653 (20) was maintained in DMEM supplemented with 10% Fetal Bovine Serum (FBS), 5 mM glutamine and 50 $\mu$g/ml gentamycin (supplemented DMEM) at 37°C in a humidified 10% $CO_2$ atmosphere. Hybridomas were initially grown in supplemented DMEM under HAT selection (100 $\mu$M hypoxanthine, 400 nM aminopterin, 16 $\mu$M thymidine), transferred to supplemented DMEM under HT selection (100 $\mu$M hypoxanthine and 16 $\mu$M thymidine) and later grown solely in supplemented 10% FBS/DMEM. The human fibrosarcoma cell line, FS 1,2,3 and epitheloid carcinoma cell line, HeLa, were grown in 10% FBS/DMEM plus supplements at 37°C and 10% $CO_2$. All other human cell lines were grown in RPMI 1640 medium supplemented with 10% FBS, 5 mM glutamine and 50 $\mu$g/ml gentamycin at 37°C and 5% $CO_2$. All cell lines used in this study are listed in Table 2.

Human umbilical vein endothelial cells (HUVEC, passage number 2-4) were maintained as a monolayer on fibronectin-coated dishes in M199 medium, 20% FBS (Hyclone Laboratories, Inc., Logan, UT; LPS = 0.025 ng/ml), 5 mM glutamine, 50 $\mu$g/ml gentamycin, 100 $\mu$g/ml endothelial growth supplement (Biomedical Technologies, Inc., Stoughton, MA) and 100 $\mu$g/ml heparin at 37°C and 5% $CO_2$. For stimulation, 5 U/ml of recombinant human IL-1$\beta$ (Boehringer Mannheim, Indianapolis, IN), 10 $\mu$g/ml of LPS (Sigma Chemical Co., St. Louis, MO), 20 ng/ml of recombinant human TNF-$\alpha$ (Genzyme, Boston, MA) or $10^3$ U/ml of recombinant IFN-$\gamma$ (Genzyme) was added to the medium at either 4 or 24 h before harvesting. Stimulation of HUVEC was monitored by flow cytometry analysis of ICAM-1 on treated and untreated cells.

Peripheral blood mononuclear cells (PBMC) were obtained by dextran sedimentation and Ficoll-Hypaque (1.077) centrifugation as described (15). Granulocytes were recovered from the cell pellet; contaminating erythrocytes were removed by hypotonic lysis. Lymphocytes were enriched by incubating the PBMC in 10% FBS/RPMI 1640 on tissue culture-treated plastic Petri dishes for 2 h and saving the nonadherent cells. To enrich for T lymphocytes, the nonadherent cells were passed through nylon wool (21). NK cells were further isolated from plastic and nylon wool nonadherent mononuclear cells by Percoll (Pharmacia Fine Chemicals, Piscataway, NJ) gradient centrifugation as described (22). $CD3^+$ cells were removed by labelling with CD3 mAb (OKT3) and removing the mAb bound cells by rosetting with magnetic beads (Dynal; Robbins Scientific, Mountain View, CA) coated with $F(ab')_2$ goat anti-mouse IgG and IgM (Tago Inc., Burlingame, CA). Immunofluorescence flow cytometry showed the purified NK cells to be >75% $CD16^+$ with few (<10%) contaminating $CD3^+$ cells. PHA blasts were prepared from isolated PBMC, incubated in supplemented RPMI, plus 10% FBS and 10 $\mu$g/ml PHA-P (Sigma Chemical Co.) and assayed at the indicated times (23). Plastic adherent monocytes were either analyzed immediately or cultured in vitro for 10 d to induce differentiation towards macrophage-like cells (24). The adherent cells were removed with HBSS/EDTA and surface antigen expression examined by immunofluorescence flow cytometry.

*cDNA and Transfection.* ICAM-1 and ICAM-2 cDNAs in the transient expression vector CDM8 (13, 17) or vector alone (mock) were transfected into COS cells using DEAE-dextran (25). 3 d after transfection, cells were detached with 10 mM HBSS/EDTA, washed three times in 10%FBS/RPMI 1640 and then used for immunization, flow cytometric analysis, $^{125}$I-labeling, or binding to LFA-1–coated plates. Cells were washed twice with PBS, pH 7.3, before either immunization or $^{125}$I-labeling.

*Development of ICAM-2 Hybridomas.* Transfected COS cells expressing ICAM-2 were used to immunize 3–12-wk-old BALB/c female mice (Charles River Laboratories, Wilmington, MA). Immunizations ($10^5$–$10^6$ cells/i.p. immunization) were performed four times at 3-wk intervals. 3 d before fusion with the murine myeloma P3X63Ag8.653, the mice were injected both i.p. and i.v. with $5 \times 10^5$ COS cells transiently expressing ICAM-2. These transfectants were tested for ICAM-2 expression by specific binding to LFA-1. The protocol for fusion and subsequent maintenance of hybridomas is as previously described (26). Differential reactivity to ICAM-2 transfected COS cells and untransfected cells was used initially to screen for ICAM-2 mAbs. Initial screening was performed by ELISA, followed by flow cytometric analysis of putative ICAM-2 reactive hybridoma supernatants. Positive mAbs were then screened for reactivity to cell lines known to be either positive (SKW3) or negative (HeLa) for ICAM-2 by Northern blotting analysis (17). MAbs selected for further analysis were cloned twice by limiting dilution and isotyped by ELISA using affinity purified antibodies to mouse immunoglobulins (Zymed Immunochemicals, San Francisco, CA).

*Immunohistochemical Staining.* Fresh tissues were received at the Department of Surgical Pathology at Thomas Jefferson University and snap-frozen in liquid nitrogen. The tissues were stored at −70°C until use. Immunohistological staining was carried out following the alkaline phosphatase (AP) anti-alkaline phosphatase procedure (27). Briefly, 7 μm frozen tissue sections were air-dried overnight and fixed in acetone for 10 min. ICAM-1 (RR1/1) and ICAM-2 (CBR-IC2/1) mAb were applied at 1/12,000 and 1/2,000 dilutions of ascites fluid, respectively, for 30 min followed by brief washing in Tris-buffered saline, pH 7.6. As a negative control, mouse serum at a 1/5,000 dilution was applied. After washing, the sections were incubated with a 1/40 dilution of rabbit anti–mouse Ig mAb (Dakopatts, Carpinteria, CA) for 30 min. Finally, after intermittent washing, the cells were incubated with APAAP-complex (anti-AP mouse mAb preincubated with AP). The last two steps were repeated in order to enhance the sensitivity of this procedure. Bound alkaline phosphatase was visualized using new fuchsin (Sigma Chemical Co.) as substrate. Levamisole was applied in order to block endogenous alkaline phosphatase activity and Meyer's acid hematoxylin (Sigma Chemical Co.) was used as counterstain.

*Flow Cytometric Analysis.* Adherent cells were removed with 10 mM HBSS/EDTA, washed with PBS/2% FBS and 50 μl of a 0.5–1.0 × $10^6$ cells/ml suspension was added to either 50 μl of mAb supernatant or 50 μl of a 1/200 dilution of mAb containing ascites fluid. After 45 min incubation at 4°C, the cells were washed and incubated with 100 μl of a 1/20 dilution of FITC-labeled goat anti–mouse Ig (Zymed Immunochemicals) for 45 min at 4°C. The cells were rewashed and fixed in 1% paraformaldehyde/PBS. Samples were analyzed using an Epics V (Coulter Diagnostics, Hialeah, FL) flow cytometer. As both primary and secondary mAb were used at saturating concentrations, membrane antigen expression could be quantitated as a measure of mean fluorescence intensity using EPICS Immuno-Brite fluorescent beads (Coulter Diagnostics) to calibrate the cytometer, and X63 control antibody staining used to subtract nonspecific fluorescence.

*Surface Iodination.* Surface labeling of cells with $^{125}I$ was performed as described using Iodogen (Pierce Chemical Co., Rockford, IL) (28). Cells were labeled with $^{125}I$ (1.0 mCi Na $^{125}I$; Amersham Corp., Arlington Heights, IL) and lysed for 45 min at 4°C in 1 ml of lysis buffer (10 mM Tris HCl pH 8.0, 150 mM NaCl, 1% Triton-X-100, 1% hemoglobin, 1 mM iodoacetamide, 1 mM PMSF, 0.24 TIU/ml aprotonin, 0.025% azide). Nuclei and insoluble debris were removed by centrifugation at 14,000 *g* for 20 min and lysates precleared overnight at 4°C with 100 μl of packed bovine IgG coupled-Sepharose. The lysate was then incubated with 30 μl packed mAb bound to Sepharose for 2 h. The beads were washed four times in 25 mM Tris HCl pH 8.0, 150 mM NaCl, 0.1% Triton-X-100, twice in 25 mM Tris pH 8.0, 150 mM NaCl, and once in 50 mM Tris pH 8.0. The beads were then treated with an equal volume of 2 × SDS-PAGE sample buffer, boiled for 2 min and analyzed on 8% vertical slab polyacrylamide gels as previously described (29). Proteins were visualized by autoradiography. Treatment of samples with N-glycanase (Genzyme Corp.) was as previously described (33), using a concentration (3 U/ml) determined to give optimal cleavage of all N-linked oligosaccharides from the peptide backbone.

*Purification of LFA-1.* LFA-1 was purified from JY lysates on TS2/4-Sepharose as described previously (30). The LFA-1 bound to TS2/4-Sepharose was eluted with 50 mM triethylamine pH 11.5, 150 mM NaCl, 2 mM $MgCl_2$, and 1% octyl β-D-glucopyranoside (OG). Samples were neutralized and stored frozen at −70°C.

*Adhesion Assay.* Purified LFA-1 in 1% OG was diluted 1/10 or 1/20 in 25 mM Tris HCl pH 8.0, 150 mM NaCl, 2 mM $MgCl_2$ (TSM) and 50 μl absorbed onto 96-well polystyrene microtitre plates (Linbro-Titertek; Flow Laboratories, McLean, VA) for 2 h at room temperature. Nonspecific binding sites were blocked for 2 h at room temperature with TSM/1% BSA and then washed twice with PBS/5% FBS/2 mM $MgCl_2$/0.5% HSA (assay media). Specific inhibition of LFA-1 was achieved by an incubation for 30 min at room temperature with a 1/200 dilution of TS1/22 ascites. The number of LFA-1 sites/microtitre well was determined using saturating amounts of $^{125}I$-TS1/22 mAb and calculated assuming monovalent binding of the mAb. Site numbers are expressed per $\mu m^2$; the surface area of a microtitre well was determined to be 3.85 × $10^7$ $\mu m^2$.

Cell lines were harvested, washed once in 10% FBS/RPMI 1640, resuspended and labeled with 15 μg/mL of 2′,7′-bis-(2-carboxyethyl)-5(and-6) carboxyfluorescein (BCECF; Molecular Probes, Inc., Eugene, OR) for 30 min at 37°C. After washing twice in 10% FBS/RPMI 1640, cells were counted and resuspended in assay media. Adhesion of cell lines to LFA-1–coated plates (31) or endothelial cell monolayers (15) has been described previously. Briefly, confluent endothelial cell monolayers in 96-well plates were treated with a 1/200 dilution of the appropriate ascites for 45 min at 37°C and then unbound mAb was removed by washing before the binding assay. MAb pretreatment of cells consisted of incubation with a 1/200 dilution of ascites for 45 min at 4°C, after which 0.75–1.0 × $10^5$ cells were transferred to each well. Cells were allowed to settle and adhere to either the solid phase LFA-1 or the endothelial monolayers for 1 h at 37°C. Washing consisted of 6 aspirations with either a 21-gauge needle (monolayers) or a 25-gauge needle (LFA-1–coated plates). Wells were examined microscopically before and after washing to assess the evenness of cell settling and damage to the endothelial monolayer. Damage to the monolayer was never significant (<5% area). Fluorescence was directly quantitated from the 96-well plates using a Pandex fluorescence concentration analyzer (Baxter Healthcare Corp., Mundelein, IL).

Adherence of ICAM-$2^+$ COS cell transfectants to LFA-1–coated wells was performed as previously described (31). In short, 5 × $10^4$ $Na_2{}^{51}CrO_4$-labeled transfectants were bound to LFA-1–coated plates for 1 h at room temperature, and washed with four aspirations through a 26-gauge needle. Bound cells were eluted and quantitated by γ counting.

*Aggregation Assay.* A qualitative aggregation assay was carried out as described (32). Briefly, 50 μl of a cell suspension (2 × $10^6$/ml) in 10% FBS/RPMI 1640 was preincubated with a 1/100 dilution of ascites (1/200 final concentration) for 45 min at 4°C. These cells were then stimulated with 50 ng/mL of PMA and added to a flat bottom 96-well microtiter plate (Becton Dickinson, Lincoln Park, NJ). Cells were incubated for 2–6 h at 37°C, viewed with an inverted microscope and aggregation scored visually. Because these two cell lines aggregate with different kinetics, the length of the assay was varied to maximize PMA-induced aggregation (JY: 2 h; SKW3: 5 h). Scores ranged from 0 to 5, where 0 indicates essentially no cells were clustered; 1 indicates less than 10% of cells were in clusters; 2 indicates between 10–50% of cells were in aggregates; 3 indicates 50–100% of cells were in aggregates; 4 indicates nearly 100% of cells were in large clusters of aggregates; and 5 indicates that all the cells were in very compact aggregates. Photomicrographs of aggregating cells were taken using a Nikon Diaphot-TMD inverted microscope (Nippon Kogaku, Tokyo, Japan) and phase contrast optics.

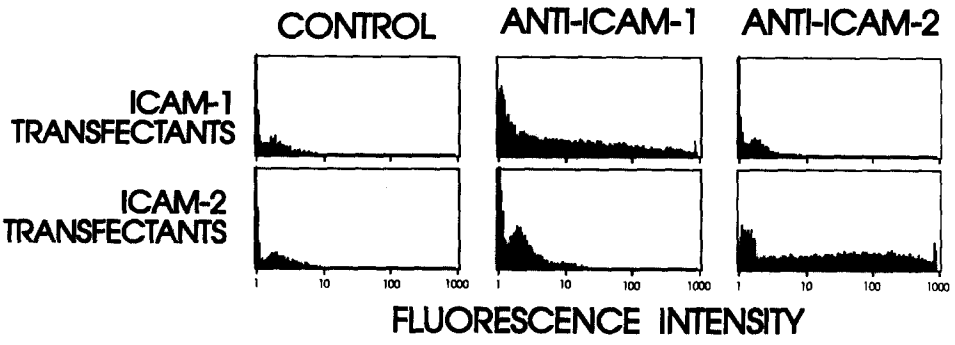


**Figure 1.** Flow cytometry analysis of COS cells transfected with either ICAM-1 or ICAM-2 cDNA. Transfected COS cells were labeled with either nonbinding control mAb X63, mAb RR1/1 (anti-ICAM-1) or mAb CBR-IC2/1 (anti-ICAM-2). CBR-IC2/2 gave an identical pattern of staining.

## Results

*Development of Anti-ICAM-2 MAbs.* Hybridomas producing anti-ICAM-2 mAb were generated by the fusion of myeloma cells with spleen cells from mice immunized with COS cells transfected with ICAM-2 cDNA. Two mAb, CBR-IC2/1 (IgG2a) and CBR-IC2/2 (IgG2a) were produced which bound specifically to COS cells transfected with ICAM-2 cDNA but not to COS cells transfected with ICAM-1 cDNA (Fig. 1) or to COS cells transfected with CDM8 vector alone (data not shown).

*Biochemical Characterization of ICAM-2.* Immunoprecipitation of $^{125}$I labeled ICAM-2$^+$ COS cell lysates showed that under nonreducing conditions, both anti-ICAM-2 mAb immunoprecipitated a broad band of $M_r$ 54–68,000 from the ICAM-2 transfectants (Fig. 2 *A*, lanes *5* and *6*) and failed

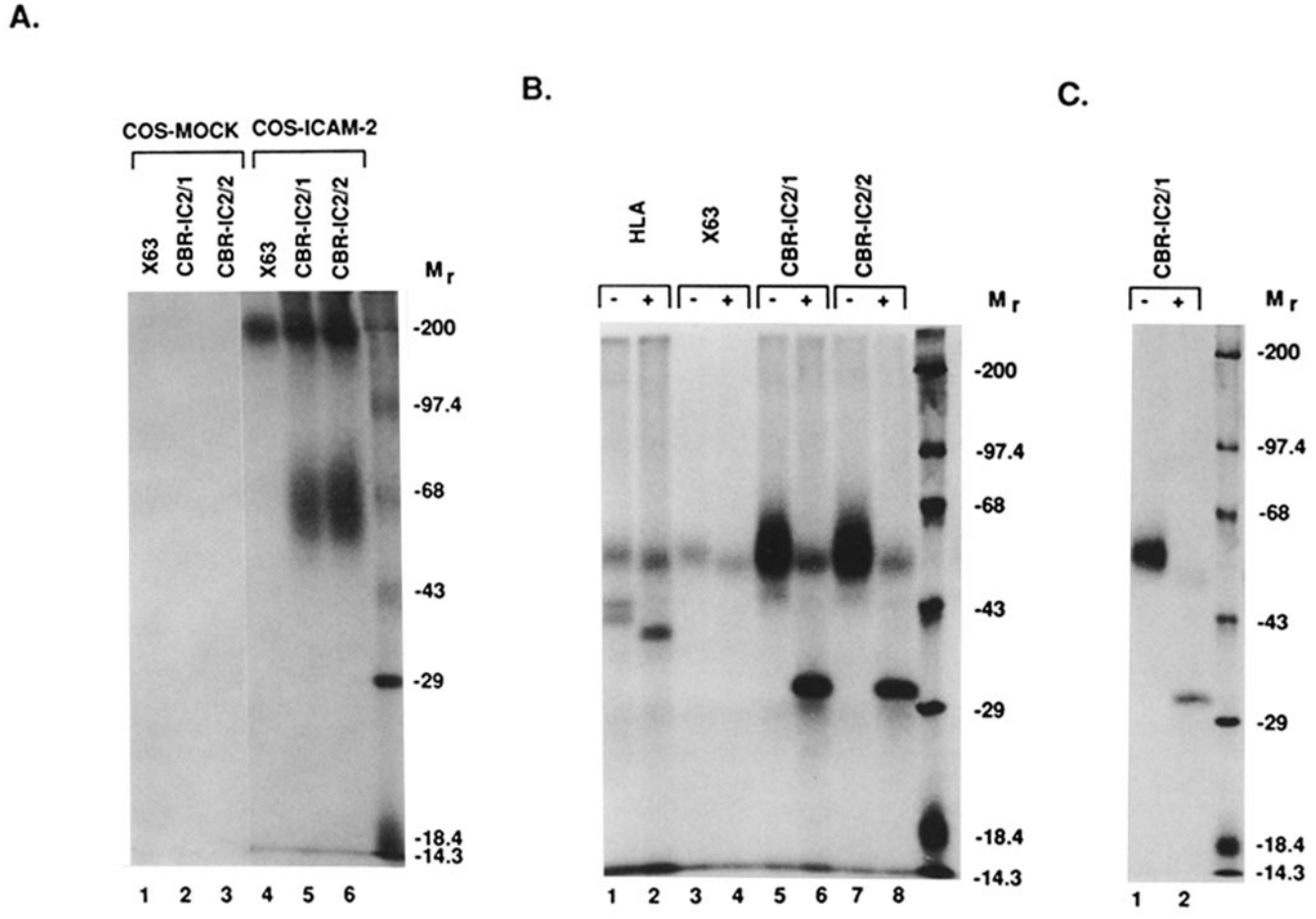


**Figure 2.** Immunoprecipitation of ICAM-2. (*A*) $^{125}$I-labeled COS cell lysates were immunoprecipitated with either nonbinding control mAb X63 or mAb CBR/IC2/1 (anti-ICAM-2) or mAb CBR-IC2/2 (anti-ICAM-2). (*B*) $^{125}$I-labeled COS cell lysates treated with (+) or without (−) N-glycanase, and immunoprecipitated with either positive control mAb W6/32 (anti-HLA-A, B, C), nonbinding control mAb X63, mAb CBR-IC2/1 (anti-ICAM-2) or mAb CBR-IC2/2 (anti-ICAM-2). MHC Class I contains one N-linked carbohydrate and acts as a control for the N-glycanase treatment. (*C*) $^{125}$I-labeled HUVEC lysates immunoprecipitated with mAb CBR-IC2/1 (anti-ICAM-2) and treated with (+) or without (−) N-glycanase, as indicated. All immunoprecipitates were analyzed by 8% SDS polyacrylamide nonreducing (*A*) or reducing (*B* and *C*) gels and subjected to autoradiography; reduced mol wt standards are shown in the far right lane.

**Table 1.** *Distribution of ICAM-1 and ICAM-2 on Normal Human Tissues**

| Tissue | ICAM-1 | ICAM-2 |
|---|---|---|
| All vascular endothelium | + | + |
| Lymph Node/Tonsil/Spleen | | |
| Follicle mantle cells | + | –‡ |
| Germinal center cells | + | –§ |
| Interfollicular/paracortical T cells | – | – |
| Follicular dendritic cells (FDC) | + | – |
| Interdigitating cells (IDC) | – | – |
| Starry sky macrophages | + | – |
| High endothelial venules (lymph node, tonsil) | + | + |
| Tonsil | | |
| Oral mucosa | + | – |
| Crypt epithelia | + | – |
| Granulocytes | – | – |
| Fibrocytes/fibroblasts | (+) | – |
| Spleen | | |
| Marginal zone cells | + | – |
| Sinus lining cells | + | + |
| Thymus | | |
| Hassall's corpuscles | – | – |
| Cortical thymocytes | (+) | – |
| Medullary thymocytes | + | – |
| Skin | | |
| Epidermal cells, Langerhans' cells, Melanocytes, Sweat gland cells | – | – |
| Fibrocytes/fibroblasts | (+) | – |
| Lungs | | |
| Alveolar lining cells, pneumocytes type I and II, alveolar macrophages | + | – |
| Capillary endothelial cells | + | + |
| Liver | | |
| Hepatocytes | + | – |
| Kupffer's cells | + | (+) |
| Sinus lining cells | + | (+) |
| Bile duct cells | – | – |
| Kidney | | |
| Endothelial cells of the glomerulum | + | + |
| Cells of Bowman's capsule, basal membrane of the glomerulum capillaries, tubular cells | – | – |
| Intertubular spindle cells | + | + |
| Small Intestine | | |
| Peyer's patches | + | – |
| Lymphocytes of the mucosal stroma | + | – |

to immunoprecipitate from mock transfectants (Fig. 2 *A*, lanes *2* and *3*). Under reducing conditions, ICAM-2 migrates with a $M_r$ of 55–65,000 (Fig. 2 *B*, lanes *5* and 7). To evaluate the contribution of glycosylation to this $M_r$, samples were treated with N-glycanase, thereby removing all N-linked oligosaccharides (33). Treatment with N-glycanase resulted in reduction of the ICAM-2 band to an approximate 31,000 $M_r$ (Fig. 2 *B*, lanes *6* and *8*), which corresponds closely to the predicted mature peptide backbone of 28,393 $M_r$. Therefore, ICAM-2, like ICAM-1, is a heavily N-glycosylated protein.

Immunoprecipitation of ICAM-2 from various cell lysates confirmed the results obtained with the COS cell transfectants. Cultured HUVEC represent the most abundant source of ICAM-2 as determined by mRNA expression (17) or by cell surface expression (Table 2). Immunoprecipitation of ICAM-2 from HUVEC lysates revealed a species migrating with an $M_r$ of 55–65,000 under reducing conditions (Fig. 2 *C*, lane *1*). Deglycosylated ICAM-2 from HUVEC (Fig. 2 *C*, lane *2*) was the same $M_r$ as from transfected COS cells. Unlike ICAM-1, little variation in $M_r$ among different cell types was seen for ICAM-2, as immunoprecipitations from both SKW3 and JY lysates yielded identical results to those seen with HUVEC lysates (data not shown).

*Tissue Distribution of ICAM-2.* Immunohistochemical staining of frozen tissue sections revealed ICAM-1 and ICAM-2 to have distinct patterns of distribution (Table 1, Fig. 3). Normal fetal (21 wk) and adult tissues showed a pattern of ICAM-1 staining similar to that previously reported (34, 35). In contrast to ICAM-1, the distribution of ICAM-2 was restricted to the endothelium and some lymphoid cells. ICAM-2 was expressed on all blood vessel endothelium, including high endothelial venules (Fig. 3 *D*), and expression was consistently stronger than that seen for ICAM-1. Examination of germinal centers of lymphoid tissue revealed ICAM-2 to be absent on most cells (Fig. 3 *B* and *D*). In the spleen, although ICAM-2 was virtually absent on all lymphocytes in the white pulp, strong reactivity was seen on the sinus lining cells of the red pulp (Fig. 3 *B*). In addition to the marginal reactivity of follicular mantle cells, ICAM-2 was found to be strongly expressed on small clusters of lymphocytes within germinal centers of both spleen and tonsil (Fig. 3 *D*). As expected, anti–ICAM-1 mAb showed intense reactivity with the germinal centers of lymphoid follicles, most likely representing reactivity with B cells and follicular dendritic cells, while the follicular mantle and marginal zones of the follicle showed weaker reactivity (Fig. 3 *A* and *C*). ICAM-1 was highly expressed on tonsil surface and crypt epithelium (Fig. 3 *C*),

* Organs studied: lymph node, tonsil, spleen, thymus, heart, brain, peripheral nerve tissue, skin, lungs, stomach, small and large intestine, liver, kidney, ovary, uterus, mammary gland, adrenal gland, and thyroid gland. Strong expression is denoted as "+" and lack of expression is denoted as "–"; "(+)" indicates a partial reactivity. Where not indicated, tissues were negative for both ICAM-1 and ICAM-2.

‡ Marginal reactivity for ICAM-2 was observed for follicular mantle cells in the spleen.

§ Small foci of germinal center lymphocytes were positive for ICAM-2.

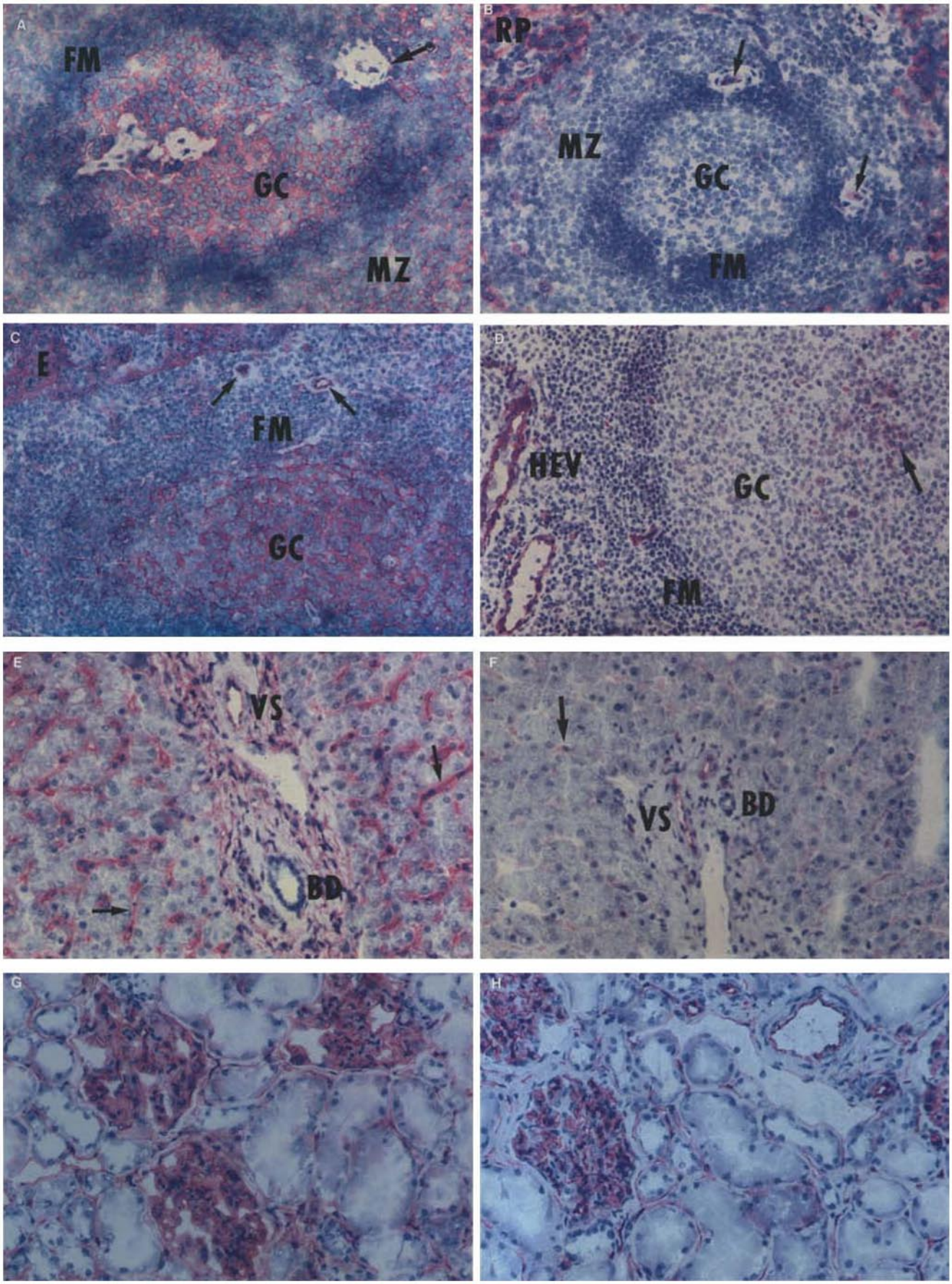
A
FM
GC
MZ
B
RP
MZ
GC
FM
C
E
FM
GC
D
HEV
GC
FM
E
VS
BD
F
VS
BD
G
H

whereas ICAM-2 was not. Fetal thymus expressed high levels of ICAM-1 in the medulla and only low levels in the cortex, while ICAM-2 reactivity was confined to vessel endothelium. In the cortical region ICAM-1 expression was primarily focal on dendritic and epithelial cells, whereas high levels of ICAM-1 in the medulla was localized to both the dendritic/macrophage cells and the thymocytes.

In nonlymphoid organs, several differences in expression were observed between ICAM-1 and ICAM-2 (Table 1). While macrophages, fibroblast-like cells, and dendritic cells expressed high levels of ICAM-1 in most tissues studied, ICAM-2 expression in tissues was restricted to blood vessel endothelium. Additional ICAM-2 expression was seen only in the liver and the kidney. In the liver, ICAM-2 was weakly expressed on Kupffer cells and some sinusoidal lining cells (Fig. 3 *F*). ICAM-1 by comparison was strongly expressed by Kupffer cells and sinusoidal lining cells (Fig. 3 *E*). In kidney, the glomerular capillary endothelium expressed ICAM-2, as did the intertubular spindle cells (Fig. 3 *H*). The ICAM-2 expression in kidney, although weaker than ICAM-1, was similar in its distribution (Fig. 3 *G*). These exceptions aside, ICAM-2 was not present on any other tissues studied, including small and large intestine, striated and smooth muscle, brain, thyroid gland, and skin.

*Immunofluorescence Flow Cytometry of ICAM-2 Membrane Expression.* Flow cytometric analysis of human tumor cell lines and PBLs supported the results obtained in frozen tissue sections (Table 2). Resting lymphocytes and purified T cells expressed both ICAM-1 and ICAM-2 at low levels, although ICAM-2 was always significantly higher in expression than ICAM-1. The pattern of expression for ICAM-2 differed from ICAM-1 in that nearly all resting cells were ICAM-2 positive and expression increased only slightly upon PHA activation. Two-color flow cytometry revealed resting T ($CD3^+$) and B ($CD20^+$) lymphocytes to express equivalent amounts of ICAM-2 on their cell surface (data not shown). In contrast to resting lymphocytes, freshly purified monocytes showed greater ICAM expression, with ICAM-1 and ICAM-2 being generally equivalent. In vitro culturing of monocytes has been used as a method of obtaining macrophage-like $CD16^+$ cells (24). Upon culturing of monocytes to induce macrophage differentiation, ICAM-2 expression remained unchanged, whereas the inducibility of ICAM-1 was consistent with published data (34).

Expression of ICAM-2 on cell lines was coordinate with Northern blotting analysis. Lines which had been previously shown to express ICAM-2 mRNA (HUVEC, SKW3, Jurkat, BBN, Ramos, U937) or lack ICAM-2 mRNA (HeLa, FS1,2,3) showed corresponding patterns of cell surface expression (Table 2). All T and B lymphoblastoid lines examined expressed considerable ICAM-2, while other cell lines exhibited a broad range of expression. Treatment of several cell lines (HUVEC, JY, and SKW3) with phosphoinositol-phospholipase C (PI-PLC), revealed no PI-linked form of ICAM-2 as cell surface expression remained unchanged (data not shown). Mouse lymphoblastoid and fibroblastic cell lines did not react with the anti-human ICAM-2 mAb, implying that these mAb did not crossreact to murine ICAM-2.

*ICAM-2 Expression on Cultured Endothelial Cells.* Of all cell types examined, ICAM-2 was most highly expressed on endothelial cells. We examined the relative levels of ICAM expression on resting and stimulated human umbilical vein endothelial cells (Fig. 4). Resting endothelial cells showed low basal level expression of ICAM-1 and approximately 10-fold higher ICAM-2 expression. The level of ICAM-2 expression was also significantly higher than that seen for either LFA-3 or HLA-A, B, C. Upon stimulation of endothelial cells with TNF-$\alpha$, ICAM-1 expression increased after 4 h, becoming maximal after 24 h stimulation, while ICAM-2 expression remained unchanged. LFA-3 was largely unaffected by cytokine stimulation, whereas HLA-A,B,C showed slightly increased expression, as previously reported (15, 36, 37). Identical findings were obtained with a variety of other stimuli including IL-1$\beta$, LPS, and IFN-$\gamma$ (data not shown). ICAM-2 therefore was found to be constitutively expressed at high levels on HUVEC and, unlike ICAM-1, was not increased by stimulation with inflammatory mediators.

*Functional Characterization of ICAM-2 MAb.* To determine whether CBR-IC2/1 and CBR/IC2/2 could inhibit ICAM-2–LFA-1 interaction, binding of ICAM-$2^+$ COS cells to purified LFA-1 was performed in the presence of these mAb (Fig. 5). A high percentage of transfected cells bound to purified LFA-1 in the presence of control mAb W6/32, and this was totally inhibitable by an anti-LFA-1 mAb. Of the

**Figure 3.** Photomicrograph of immunohistochemical alkaline phosphatase anti-alkaline phosphatase (APAAP) staining of frozen tissues with anti-ICAM-1 (RR1/1) and anti-ICAM-2 (CBR-IC2/1) mAb (magnification ×200). (*A*) Staining of spleen with anti-ICAM-1 mAb. Note that the germinal center (GC) cells, follicular mantle (FM) cells and marginal zone (MZ) cells are positive for ICAM-1. Endothelium of small vessels is also positive (*arrow*). (*B*) Staining of spleen with anti-ICAM-2 mAb. With the exception of very faint staining of the follicular mantle (FM) lymphocytes, no staining of the white pulp is observed including germinal center (GC) and marginal zone (MZ) cells. The red pulp (RP) shows intense staining of the sinus lining cells. Small vessel endothelium is stained (*arrows*). (*C*) Normal tonsil stained with anti-ICAM-1 mAb. The germinal center (GC) cells show strong reactivity, whereas the follicular mantle (FM) cells are only weakly reactive. Virtually all vascular endothelium, including high endothelial venules, are positive (*arrows*). ICAM-1 is also present on the surface and crypt epithelium (E) of tonsil. (*D*) Normal tonsil stained with anti-ICAM-2 mAb. Note that virtually all vascular endothelium is positive, including high endothelial venules (HEV). Small clusters of germinal center (GC) lymphocytes are also positive for ICAM-2 (*arrow*). The follicular mantle (FM) cells show negative to faint reactivity. Epithelium is negative (not shown). (*E*) Normal liver stained with anti-ICAM-1 mAb. Kupffer cells and sinusoidal endothelium are stained (*arrows*). The endothelium of the vessels (VS) in the portal fields are also positive. Liver epithelium and bile ducts (BD) are negative. (*F*) Normal liver stained with anti-ICAM-2 mAb. Sinuoidal endothelium is largely negative for ICAM-2 and only weak reactivity is found for Kupffer cells (*arrow*). Positive staining is found for the endothelium of the vessels (VS) in the portal fields. Liver epithelium and bile duct (BD) epithelium are negative. (*G*) Normal kidney stained with anti-ICAM-1 mAb. Note that the endothelium of all glomerular capillaries is positive. Some reactivity is also observed with the intertubular spindle cells. (*H*) Normal kidney stained with anti-ICAM-2 mAb. Note the pronounced staining of all glomerular capillaries. Reactivity to intertubular spindle cells is also seen.

**Table 2.** *Relative Surface Antigen Expression of ICAMs by Immunofluorescence Flow Cytometry*

| Cell line/type | Specific linear fluorescence intensity* | | |
|---|---|---|---|
| | ICAM-1 | ICAM-2 | HLA |
| Lymphocytes | 13 | 45 | 840 |
| T lymphocytes | 14 | 40 | 920 |
| 1 day PHA-blasts | 64 | 40 | 1,100 |
| 4 day PHA-blasts | 200 | 55 | 1,600 |
| 7 day PHA-blasts | 70 | 32 | 1,100 |
| Monocytes | 72 | 87 | 990 |
| Cultured monocytes | 293 | 80 | 1,200 |
| Neutrophils | 5 | 0 | 275 |
| NK cells | 12 | 32 | 1,050 |
| Erythrocytes | 0 | 0 | 0 |
| T lymphoblastoid | | | |
| SKW3 | 0 | 114 | 670 |
| Jurkat | 21 | 181 | 200 |
| Sup T | 57 | 178 | 180 |
| Molt 4 | 28 | 240 | 253 |
| B lymphoblastoid | | | |
| JY | 125 | 130 | 1,600 |
| Ramos | 190 | 260 | 670 |
| Raji | 282 | 72 | 468 |
| Daudi | 260 | 135 | 260 |
| ER-LCL | 150 | 110 | 705 |
| BBN | 100 | 60 | 215 |
| RPMI 8866 | 146 | 117 | 618 |
| Monocytic | | | |
| U937 | 31 | 29 | 220 |
| HL60 | 0 | 23 | 268 |
| Melanomas | | | |
| BK | 181 | 8 | 265 |
| RPMI 7591 | 194 | 0 | 710 |
| Erythroleukemic | | | |
| K562 | 155 | 95 | 6 |
| HEL | 58 | 118 | 950 |
| Miscellaneous‡ | | | |
| HUVEC | 41 | 470 | 260 |
| ZR-75-1 | 105 | 30 | 105 |
| Hep G2 | 142 | 17 | 140 |
| HeLa | 225 | 0 | 155 |
| RD3/5 | 0 | 11 | 208 |
| FS1,2,3 | 225 | 0 | 645 |
| A-172 | 0 | 0 | 385 |
| L428 | 835 | 169 | 16 |

two anti-ICAM-2 mAb, CBR-IC2/1 caused slight inhibition, whereas CBR-IC2/2 completely blocked adherence to levels seen in the presence of anti-LFA-1 mAb. A combination of both anti-ICAM-2 mAb gave no additional inhibition to that seen when using CBR-IC2/2 alone. Both mAb were used at saturating concentrations, and this inhibitory effect could be diluted out. Similar results were obtained using mouse L cells stably expressing human ICAM-2, demonstrating the ability of mAb CBR-IC2/2 to completely inhibit ICAM-2 interaction was purified LFA-1 (data not shown). CBR-IC2/1 and CBR/IC2/2 were determined to recognize nearby but distinct epitopes on ICAM-2, because although CBR-IC2/2 would completely block CBR-IC2/1 binding, the latter could only partially block the former (data not shown).

*Effect of Anti-ICAM-2 MAbs on Homotypic Aggregation.* We examined the ability of anti-ICAM-1 and anti-ICAM-2 mAb to inhibit LFA-1-dependent homotypic aggregation of several cell lines (Table 3 and Fig. 6). PMA-induced aggregation of JY, an EBV-transformed B lymphoblastoid cell line, was previously found to be inhibitable almost completely by the blocking anti-ICAM-1 mAb, RR1/1 (10). Alone, anti-ICAM-1 mAb was found to inhibit most aggregation (Fig. 6 *C*), but when used in conjunction with anti-ICAM-2 mAb aggregation was inhibited completely (Fig. 6 *E*); to the same extent as with anti-LFA-1 mAb (Fig. 6 *F*). Consistent with the functional characterization of both CBR-IC2/1 and CBR-IC2/2, when the anti-ICAM-2 mAb were used separately with RR1/1, only CBR-IC2/2 inhibited aggregation. Aggregation was not inhibited by the anti-ICAM-2 mAb alone (Fig. 6 *D*); this is due to the presence of ICAM-1 and the overriding role it plays in LFA-1-dependent aggregate formation of this cell line. PMA treatment of cells resulted in little change in surface expression of either ICAM-1, ICAM-2, or LFA-1 during the course of the assay (data not shown). After 12–24 h however, ICAM-1 expression increased and ICAM-2 showed a slight decrease.

PMA-induced aggregation of SKW3 was shown to be LFA-1-dependent, but ICAM-1-independent (Table 3). This is consistent with previously published reports (10). Anti-ICAM-2 mAb had no effect on SKW3 aggregation either alone or in combination with RR1/1 (Table 3). Given the ability of RR1/1 and CBR-IC2/2 to inhibit ICAM-1 and ICAM-2-dependent binding by other cells, these results suggest the presence of a third ligand for LFA-1 on SKW3.

*Effect of Anti-ICAM-2 MAbs on Cell Line Binding to LFA-1.* To better define this putative third LFA-1 ligand, binding of

* Membrane expression determined by immunofluorescence flow cytometry with RR1/1 for ICAM-1, CBR-IC2/1 for ICAM-2, and W6/32 for HLA-A,B,C. Values are determinative of at least two experiments. Fluorescent beads were used to calibrate the cytometer such that one unit was approximately $10^3$ fluorescein equivalents (Coulter Diagnostics).

‡ Miscellaneous cell lines include: Human umbilical vein endothelial cells, HUVEC; human breast carcinoma, ZR-75-1; human hepatocellular carcinoma, Hep G2; human epitheloid carcinoma cell line, HeLa; human rhabdomyosarcoma, RD 3/5; human fibrosarcoma, FS 1,2,3; human glioblastoma, A-172; and the Reed-Sternberg line, L428.

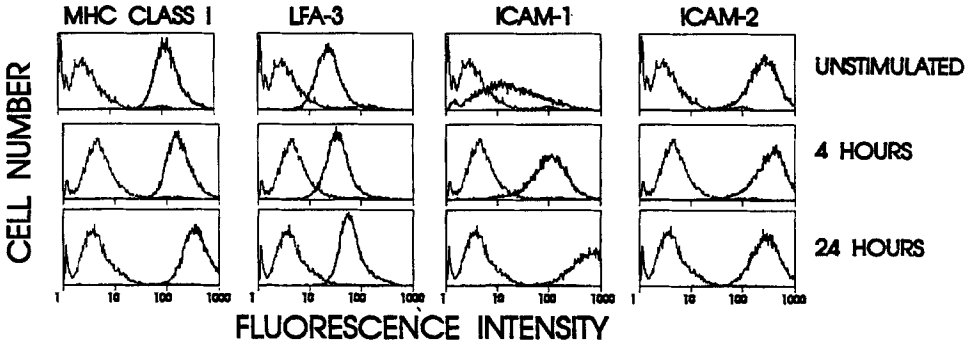


**Figure 4.** Immunofluorescence flow cytometry analysis of HUVEC before and after TNF-α stimulation. HUVEC were stimulated for the indicated length of time with 20 ng/mL TNF-α and then labeled with either mAb W6/32 (anti-HLA-A,B,C), mAb TS2/9 (anti-LFA-3), mAb RR1/1 (anti-ICAM-1), mAb CBR-IC2/1 (anti-ICAM-2), or nonbinding control mAb X63 (*thin lines*), and then followed by FITC anti-mouse Ig.

**Table 3.** *Inhibition of PMA-induced Aggregation with LFA-1, ICAM-1 and ICAM-2 mAb**

| | Aggregation index‡ | | | | | |
|---|---|---|---|---|---|---|
| Cell type | Control | αLFA-1 | αICAM-1 | αICAM-2 | αICAM-1 + 2 | αHLA |
| JY | 4 | 0 | 1 | 4 | 0 | 4 |
| SKW3 | 4 | 0 | 4 | 4 | 4 | 4 |

* Fresh JY or SKW3 cells were preincubated at 4°C for 45 min with either no mAb (control) or 1/200 dilution of mAb containing ascites: TS1/22 (anti-LFA-1α), RR1/1 (anti-ICAM-1), CBR-IC2/1 + CBR-IC2/2 (anti-ICAM-2), RR1/1 + CBR-IC2/1 + CBR-IC2/2 (anti-ICAM-1 + 2), or W6/32 (anti-HLA-A,B,C). Cells were then stimulated with 50 ng/ml of PMA, and aggregation scored visually after either 2 h (JY) or 5 h (SKW3).
‡ Aggregation scored as described in Materials and Methods. Scores: 0, no cells clustered; 1, <10% of cells aggregating; 2, 10–50% of cells aggregating; 3, 50–100% of cells aggregating; 4, nearly 100% of cells in loose aggregates; 5, 100% of cells in very compact aggregates.

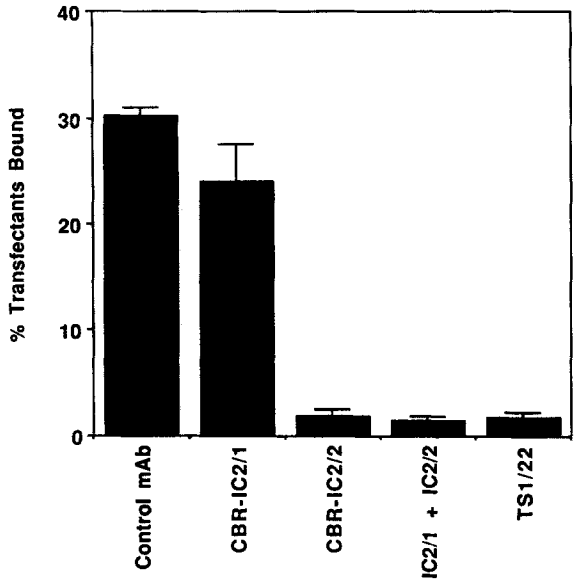


**Figure 5.** Effect of ICAM-2 mAb on binding of ICAM-2–expressing COS cell transfectants to purified LFA-1. Binding of $^{51}Cr$-labeled ICAM-2$^+$ COS cell transfectants was measured by incubating cells on LFA-1–coated microtiter wells for 60 min at room temperature and then washing four times by aspiration. Site density of LFA-1 as determined by radioimmunoassay was 1,100 sites/$\mu m^2$. Cells were incubated with saturating concentrations of control mAb W6/32 (anti-HLA-A,B,C); mAb CBR-IC2/1 (anti-ICAM-2); mAb CBR-IC2/2 (anti-ICAM-2); or mAb CBR-IC2/1 and mAb CBR-IC2/2 (anti-ICAM-2). Alternatively, the absorbed purified LFA-1 was pretreated with mAb TS1/22 (anti-LFA-1α). One representative experiment of five is shown and error bars indicate one standard deviation.

cell lines to purified LFA-1 was performed (Fig. 7). Consistent binding of all cell lines to purified LFA-1 was observed in the presence of control X63 mAb. Similar binding was achieved if no mAb was added or if other control mAbs were used (W6/32, TS2/9, TS2/16; data not shown). Paralleling the aggregation results, JY binding to purified LFA-1 was largely inhibitable with anti-ICAM-1 mAb alone, and when combined with anti-ICAM-2 mAb, binding was further inhibitable to the level seen in the presence of anti-LFA-1 mAb. Little inhibition was seen when anti-ICAM-2 mAb were used alone. SKW3 binding to LFA-1 was only slightly inhibited with a combination of mAb to ICAM-1 and ICAM-2, whereas binding was abolished with LFA-1 mAb. This third mechanism of adhesion to LFA-1 was also present at suboptimal LFA-1 sites densities and was resistant to stringent washing conditions (21-gauge needle aspiration) (data not shown). Numerous other cell lines were tested and several (Jurkat, Sup T, Ramos, Molt 4) also expressed an ICAM-1, ICAM-2–independent pathway of adhesion to LFA-1 (data not shown). Binding of unstimulated HUVEC to purified LFA-1 was found to be entirely ICAM-1 and ICAM-2–dependent. MAb to either ICAM-1 or ICAM-2 had little effect alone, whereas the combination of mAb to ICAM-1 and ICAM-2 eliminated binding as effectively as LFA-1 mAb.

*B Lymphoblastoid Cell Adhesion to HUVEC.* The adhesion of the JY B lymphoblastoid cell line to HUVEC is an ideal in vitro system in which to study LFA-1–dependent binding of lymphocytes to endothelial cells (Fig. 8). Several mechanisms of lymphocyte-endothelial adhesion exist, of

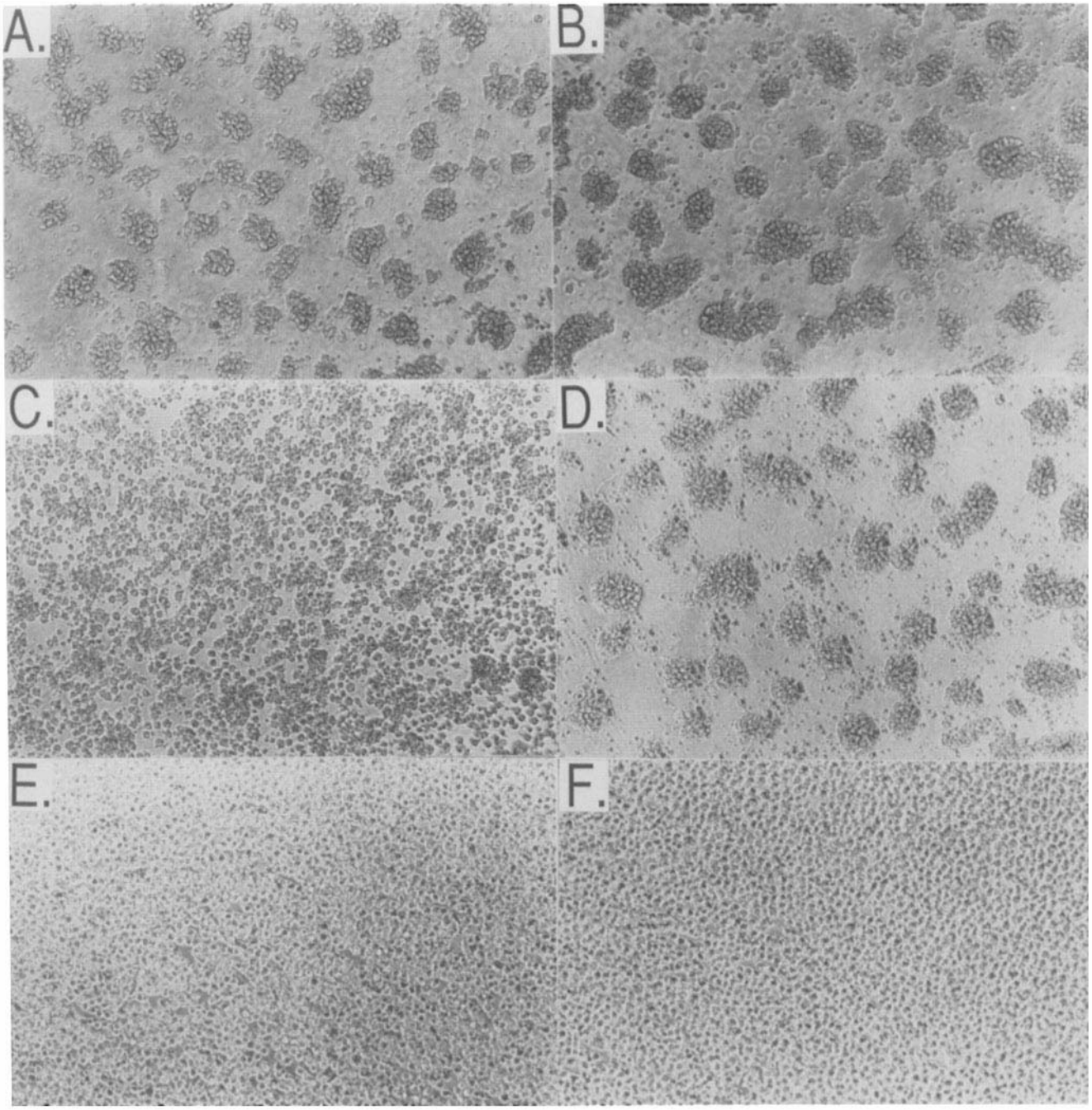


**Figure 6.** JY aggregation is completely inhibited by mAb to ICAM-1 and ICAM-2. Photomicrographs of JY cells aggregating in the presence of PMA, with: (*A*) control mAb X63; (*B*) anti-HLA framework mAb (W6/32); (*C*) anti–ICAM-1 mAb (RR1/1); (*D*) anti–ICAM-2 mAb (CBR-IC2/1 and CBR-IC2/2); (*E*) both anti–ICAM-1 and anti–ICAM-2 mAb; (*F*) anti–LFA-1$\alpha$ chain mAb (TS1/22).

which LFA-1–ICAM and VLA-4–VCAM-1 are the most important and intensively studied (1, 38, 39). Since JY cells lack $\beta$1 expression (A. de Fougerolles and T.A. Springer, unpublished observations), adhesion of these cells to endothelium allows the LFA-1–ICAM interactions to be studied independently (15) of any $\beta$1-dependent interactions, such as VLA-4–VCAM-1. The contribution of CD2–LFA-3 interactions to initial lymphocyte-endothelial cell adhesion has previously been shown to be minimal (15), and this is reflected in the inability of LFA-3 mAb to inhibit JY binding to HUVEC (Fig. 8). Previously, it was shown that binding of JY cells to HUVEC occurred via two LFA-1–dependent pathways, an inducible ICAM-1–dependent pathway and an uninducible ICAM-1–independent pathway (15). To examine if this ICAM-1–independent pathway of adhesion was due to ICAM-2, JY adhesion to HUVEC was assayed in the presence of ICAM-2

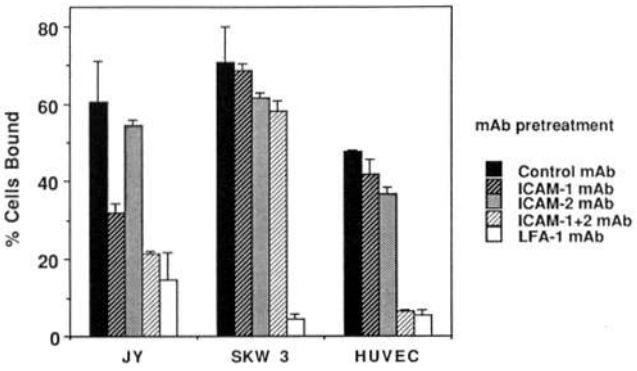


**Figure 7.** Adhesion of cell lines to purified LFA-1 reveals the presence of a novel LFA-1 ligand. Binding of BCECF-labeled cell lines was measured by incubating cells on LFA-1–coated microtiter wells for 60 min at 37°C and then washing six times by aspiration. Site density of LFA-1 as determined by radioimmunoassay was 1100 sites/$\mu m^2$. Cells were incubated in the presence of control mAb X63; Mab RR 1/1 (anti–ICAM-1); mAb CBR-IC2/1 and mAb CBR-IC2/2 (anti–ICAM-2); mAb RR1/1, mAb CBR-IC2/1 and mAb CBR-IC2/2 (anti–ICAM-1+2), or mAb TS1/22 (anti–LFA-1$\alpha$). One of eight representative experiments is shown and error bars indicate one SD.

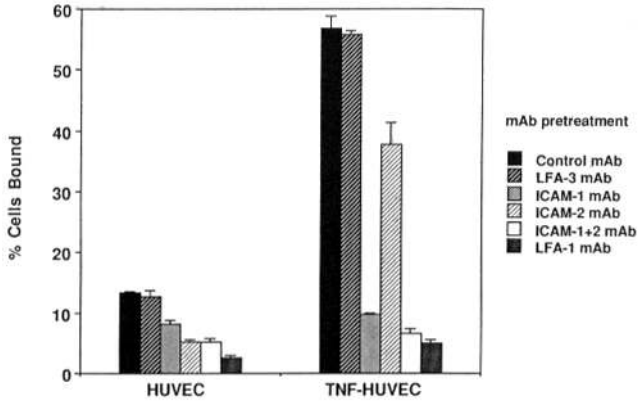


**Figure 8.** JY binding to HUVEC is solely ICAM-1 and ICAM-2–dependent. Confluent monolayers of HUVEC in 96-well plates were either untreated or stimulated for 24 h before assay with 20 ng/ml recombinant TNF-$\alpha$. BCECF-labeled JY cells were bound to the endothelial cell monolayer for 60 min at 37°C and then washed by aspiration six times. Before binding, JY cells were incubated with saturating concentrations of control mAb X63; mAb TS2/9 (anti–LFA-3); mAb RR1/1 (anti–ICAM-1); mAb CBR-IC2/1 and mAb CBR-IC2/2 (anti–ICAM-2); or mAb RR1/1, mAb CBR-IC2/1 and mAb CBR-IC2/2 (anti–ICAM-1+2). Alternatively, HUVEC were pretreated with mAb TS1/22 (anti–LFA-1$\alpha$). One representative experiment of four is shown and error bars indicate one SD.

mAb (Fig. 8). ICAM-2 mAb inhibited binding of JY cells to unstimulated endothelium more strongly than ICAM-1 mAb. Treatment of HUVEC with TNF-$\alpha$ for 24 h, resulted in a significant increase in JY adhesion (Fig. 8). This adhesion was inhibited more by ICAM-1 mAb than ICAM-2 mAb, and the combination of ICAM mAb inhibited similarly to LFA-1 mAb. The ICAM-1 component of adhesion was inducible, whereas the amount of binding seen in the presence of ICAM-1 mAb, in other words the ICAM-2 component, was constant. Studies with 24 h LPS stimulated HUVEC and 4 h TNF-$\alpha$ stimulated HUVEC yielded similar results, however, less ICAM-1–dependent binding was seen with endothelium stimulated for 4 h than 24 h (data not shown) as expected from flow cytometry data on the induction of ICAM-1. These results demonstrate that ICAM-2 is the predominant LFA-1 ligand on resting endothelial cells whereas ICAM-1 is the predominant ligand on stimulated endothelial cells.

## Discussion

ICAM-2 was initially described and characterized as a cDNA clone that encoded a counter receptor for LFA-1 (17). In this study we have reported the production of two murine mAb to ICAM-2 which allow the characterization of the ICAM-2 molecule. ICAM-2 was found to be a broad band by SDS-PAGE of $M_r$ 55–65,000 under reducing conditions. Unlike ICAM-1 (34), little variation in size was seen for ICAM-2 immunoprecipitated from different cell lines. Based on cDNA sequence, ICAM-2 has a polypeptide backbone of $M_r$ 28,393 and six potential N-linked glycosylation sites (17). Glycosylation of ICAM-2 accounted for an increase in $M_r$ of 30,000–35,000, about 5,000 $M_r$/N-linked site. Comparatively, ICAM-1 has 8 N-linked glycosylation sites, which account for about 41,000 $M_r$ of the apparent $M_r$ in SDS-PAGE. An increase of about 3,000 $M_r$/N-linked glycosylation site is more typical of glycoproteins; therefore, the N-linked carbohydrates of ICAM-1 and ICAM-2 appear unusually large. There are six and three N-linked glycosylation sites in domains 1 and 2 of ICAM-2 and ICAM-1, respectively. The ligand binding region of ICAM-1 has been localized to domain 1 (14); the comparable region in ICAM-2 is more heavily glycosylated.

The overall tissue distribution of ICAM-2 is more restricted than that of ICAM-1. ICAM-2 is restricted largely to endothelium and certain interstitial cells. Aside from vascular staining, ICAM-2 is not found at all in the thymus, while discrete clusters of ICAM-2 positive cells are seen in lymphoid tissue germinal centers. As it is difficult to distinguish between the tightly clustered follicular dendritic cells (FDC) and the surrounding germinal center B cells, this discrete staining pattern could reflect reactivity to either FDCs or B cells or a subpopulation thereof. Previous reports have demonstrated that FDCs display a unique antigenic phenotype, including expression of many adhesion molecules such as ICAM-1 (40). The expression of ICAM-2 on these cells may contribute in antigen presentation by interacting with LFA-1 on circulating lymphocytes. The distribution of ICAM-1 is consistent with previous reports (34, 35) and parallels closely that of HLA-DR. ICAM-1 is present on non-lymphoid cells, including vascular endothelium, thymic and mucosal epithelial cells, as well as B cells and follicular dendritic cells in the germinal centers of lymphoid follicles.

The distributions of ICAM-1 and ICAM-2 on cell lines parallel closely the immunohistology results. Expression of ICAM-2 was most pronounced on HUVECs, where its level on resting endothelial cells was consistently 10–15-fold higher than that for ICAM-1. ICAM-2 expression on resting lym-

phocytes was several-fold higher than that seen with ICAM-1, while monocytes expressed equivalent levels of ICAM-1 and ICAM-2. ICAM-1 is strongly expressed on melanoma and carcinoma cells (41, 42), whereas ICAM-2 is not. The weak expression of ICAM-2 observed on leukocytes by immunofluorescence flow cytometry was undetectable by immunohistochemical analysis of tissue sections, presumably due to the lower sensitivity of this technique.

The inducibility of ICAM-1 and constitutive expression of ICAM-2 have important implications for their role in inflammatory and immune responses. Previous studies have shown that although ICAM-1 was expressed at very low basal levels on endothelial cells, it was readily inducible by exposure of HUVEC to recombinant IL-1$\alpha$, IL-1$\beta$, IFN-$\gamma$, TNF-$\alpha$, and LPS (15, 36, 37). A second noninducible ligand on endothelial cells for LFA-1 was described (15) and was postulated to be ICAM-2 (17). Indeed, our studies on ICAM-2 confirmed these predictions. ICAM-2 surface expression on endothelial cells is unaffected by a variety of inflammatory cytokines. Similarly, while ICAM-1 was upregulated upon stimulation of resting lymphocytes, ICAM-2 expression was unchanged. These results point towards ICAM-1 being the major ligand for LFA-1 during inflammatory or immune responses, while ICAM-2 is of more relative importance in the unstimulated resting state or early on during a response before ICAM-1 expression is increased.

ICAM-2 is the predominant LFA-1 ligand on resting endothelium, and therefore this pathway of adhesion between lymphocytes and resting endothelium may have important consequences for normal recirculation of lymphocytes through tissue endothelium. The importance of LFA-1 in recirculation is demonstrated by the 40 to 60% reduction in normal lymphocyte migration into lymph nodes and Peyer's patches that is seen following in vivo treatment with LFA-1 mAb (43). Naive and memory T cells show distinct pathways of recirculation, as memory T cells selectively exit from blood through peripheral tissue endothelium, whereas naive T cells exit through lymph node high endothelial venules (44). ICAM-2 is an attractive candidate ligand to facilitate memory T cell recirculation as it is basally expressed at high levels on resting endothelium and memory T cells have increased LFA-1 expression (45). Similarly, resting T lymphocytes express little or no ICAM-1, and as such ICAM-2 may be important in initial T cell adhesion with antigen presenting cells that bear LFA-1 (46, 47). Indeed, in both allogeneic and autologous mixed lymphocyte reaction a role is suggested for LFA-1 ligand(s) other than ICAM-1 (48). Another immune reaction where cell-to-cell contact is required is direct cytotoxicity. Lysis of certain targets by T cells appear to occur in an ICAM-1–independent, LFA-1–dependent manner (16). It will be of interest to see what role ICAM-2 plays in these phenomena.

A mAb that blocks binding of ICAM-2 to LFA-1 was used to investigate several phenomena that were known to be LFA-1–dependent, yet ICAM-1–independent (10, 15). One such case involves homotypic aggregation of JY, an EBV-transformed B lymphoblastoid cell line. PMA-induced aggregation of this cell line, while completely LFA-1–dependent, was only partially inhibitable with mAb to ICAM-1 (10). Our results confirm these findings and extend them to show that ICAM-2 accounts for the remaining aggregates. While the ICAM-2 mAb in combination with ICAM-1 mAb can inhibit all aggregation, the ICAM-2 mAb alone has no inhibitory effect on aggregation. This observation highlights one important difference between ICAM-1 and ICAM-2, namely their relative avidity for LFA-1. By immunofluorescence ICAM-1 and ICAM-2 are expressed at similar levels on JY, yet by far the major adhesive component in homotypic aggregation and binding to purified LFA-1 is due to ICAM-1. Similar findings are seen with HUVEC binding to LFA-1 and JY adhesion to HUVEC, where although resting endothelial cells express 10-fold more ICAM-2 than ICAM-1, the effect of the anti–ICAM-2 mAb is roughly equivalent to that seen with the anti–ICAM-1 mAb. Even after 4 h TNF-$\alpha$ stimulation of endothelial cells, when ICAM-2 surface expression is still several-fold greater than ICAM-1, JY binding to HUVEC is largely inhibitable by ICAM-1 mAb (data not shown). Lastly, when comparing adhesion to purified LFA-1 of transfected COS cells expressing equivalent levels of ICAM-1 and ICAM-2, the ICAM-1 expressing cells were more resistant to increased washing shear force than were the ICAM-2 expressing COS cells (17). All of these experiments point towards ICAM-2 being the lower affinity ligand for LFA-1. At the present time the exact reason for the lower affinity of LFA-1 for ICAM-2, as compared to ICAM-1, is not known, although differences in LFA-1 binding sites, and decreased accessibility of LFA-1 for ICAM-2, due to its shorter two domain structure and increased level of glycosylation, are all plausible explanations.

Another important distinction between ICAM-1 and ICAM-2 is the spectrum of integrins with which they interact. Although ICAM-1 has been shown to interact with another leukocyte integrin, Mac-1 (49), ICAM-2 shows no detectable binding to Mac-1. Presently, LFA-1 is the only known counter-receptor for ICAM-2.

Aside from purely adhesive interactions, there may well be qualitative differences in how ICAM-1 and ICAM-2 interact with LFA-1. Previously, it had been shown that resting T cells could be actived through combination of immobilized anti-CD3 antibodies and purified ICAM-1 (50, 51). It will thus be interesting to see if ICAM-2 can exert similar effects, and ascertain if signal transduction via LFA-1 is the same when using ICAM-2 as ligand. Similarly, activation of T cells through CD3 causes a change in LFA-1 avidity from low to high, resulting in increased binding of T cells to purified ICAM-1 (30). By examining if this avidity change also extends to ICAM-2 binding, it would be possible to further dissect differences between the ICAMs. Another area where ICAM-1 and ICAM-2 could potentially differ is in their association with cytoplasmic proteins. Preferential interaction with either ICAM-1 or ICAM-2, perhaps dictated in focal adhesions by the contact distance between cells, could then result in different cytoskeletal changes affecting the overall structure and organization of the cell.

Certain LFA-1–dependent ICAM-1–independent phenomena were found not to be accountable for by ICAM-2, thus

suggesting the possibility of additional LFA-1 ligand(s). A third ligand was found to be largely responsible for SKW3 PMA-induced homotypic aggregation, and several cell lines, including SKW3, were found to bind to LFA-1–coated plastic in an ICAM-1, ICAM-2–independent manner. The strength of interaction between LFA-1 and this novel ligand appears to be intermediate between that of ICAM-1 and ICAM-2, although the relative contributions of ligand density versus affinity await the isolation and characterization of the ligand.

We thank Mr. M. Diamond for helpful discussions, Dr. D. Staunton for providing ICAM-2 cDNA, Dr. O. Carpen for natural killer cell preparation, and Mr. E. Luther for flow cytometric analysis.

This work was supported by National Institutes of Health grant CA-31798. A. de Fougerolles was a recipient of Baxter Foundation and Ryan Fellowships.

Address correspondence to Timothy A. Springer, The Center for Blood Research and Department of Pathology, Harvard Medical School, 800 Huntington Avenue, Boston, MA 02115.

*Received for publication 8 January 1991 and in revised form 18 March 1991.*

*Note added in proof:* Nortamo et al. (52) recently reported a more limited characterization of ICAM-2 using a mAb to a fusion protein. Although the reported molecular weights are similar there are major discrepancies with our reported cell distribution and previous Northern analysis (17). Nortamo et al. (52) find little or no expression of ICAM-2 on peripheral blood lymphocytes, monocytes, and the MOLT4, SKW3, and Jurkat cell lines. We find much less ICAM-1 than ICAM-2 on these cell lines whereas Nortamo et al. (52) find the reverse. In further contrast, Nortamo et al. (52) report that only 39% of unstimulated umbilical vein endothelial cells are positive for ICAM-2 and that ICAM-2 is expressed more weakly than ICAM-1.

## References

1. Springer, T.A. 1990. Adhesion receptors of the immune system. *Nature (Lond.).* 346:425.
2. Hemler, M.E. 1990. VLA proteins in the integrin family: Structures, functions, and their role on leukocytes. *Annu. Rev. Immunol.* 8:365.
3. Hynes, R.O. 1987. Integrins: A family of cell surface receptors. *Cell.* 48:549.
4. Larson, R.S., and T.A. Springer. 1990. Structure and function of leukocyte integrins. *Immunological Rev.* 114:181.
5. Kishimoto, T.K., R.S. Larson, A.L. Corbi, M.L. Dustin, D.E. Staunton, and T.A. Springer. 1989. The leukocyte integrins: LFA-1, Mac-1, and p150,95. *Adv. Immunol.* 46:149.
6. Sanchez-Madrid, F., J. Nagy, E. Robbins, P. Simon, and T.A. Springer. 1983. A human leukocyte differentiation antigen family with distinct alpha subunits and a common beta subunit: the lymphocyte function-associated antigen (LFA-1), the C3bi complement receptor (OKM1/Mac-1), and the p150,95 molecule. *J. Exp. Med.* 158:1785.
7. Anderson, D.C., and T.A. Springer. 1987. Leukocyte adhesion deficiency: An inherited defect in the Mac-1, LFA-1, and p150,95 glycoproteins. *Annu. Rev. Med.* 38:175.
8. Wardlaw, A.J., M.L. Hibbs, S.A. Stacker, and T.A. Springer. 1990. Distinct mutations in two patients with leukocyte adhesion deficiency and their functional correlates. *J. Exp. Med.* 172:335.
9. Springer, T.A., M.L. Dustin, T.K. Kishimoto, and S.D. Marlin. 1987. The lymphocyte function-associated LFA-1, CD2, and LFA-3 molecules: cell adhesion receptors of the immune system. *Annu. Rev. Immunol.* 5:223.
10. Rothlein, R., M.L. Dustin, S.D. Marlin, and T.A. Springer. 1986. A human intercellular adhesion molecule (ICAM-1) distinct from LFA-1. *J. Immunol.* 137:1270.
11. Marlin, S.D., and T.A. Springer. 1987. Purified intercellular adhesion molecule-1 (ICAM-1) is a ligand for lymphocyte function-associated antigen 1 (LFA-1). *Cell.* 51:813.
12. Simmons, D., M.W. Makgoba, and B. Seed. 1988. ICAM, an adhesion ligand of LFA-1, is homologous to the neural cell adhesion molecule NCAM. *Nature (Lond.).* 331:624.
13. Staunton, D.E., S.D. Marlin, C. Stratowa, M.L. Dustin, and T.A. Springer. 1988. Primary structure of intercellular adhesion molecule 1 (ICAM-1) demonstrates interaction between members of the immunoglobulin and integrin supergene families. *Cell.* 52:925.
14. Staunton, D.E., M.L. Dustin, H.P. Erickson, and T.A. Springer. 1990. The arrangement of the immunoglobulin-like domains of ICAM-1 and the binding sites for LFA-1 and rhinovirus. *Cell.* 61:243.
15. Dustin, M.L., and T.A. Springer. 1988. Lymphocyte function associated antigen-1 (LFA-1) interaction with intercellular adhesion molecule-1 (ICAM-1) is one of at least three mechanisms for lymphocyte adhesion to cultured endothelial cells. *J. Cell Biol.* 107:321.
16. Makgoba, M.W., M.E. Sanders, G.E. Ginther Luce, E.A. Gugel, M.L. Dustin, T.A. Springer, and S. Shaw. 1988. Functional evidence that intercellular adhesion molecule-1 (ICAM-1) is a ligand for LFA-1 in cytotoxic T cell recognition. *Eur. J. Immunol.* 18:637.
17. Staunton, D.E., M.L. Dustin, and T.A. Springer. 1989. Functional cloning of ICAM-2, a cell adhesion ligand for LFA-1 homologous to ICAM-1. *Nature (Lond.).* 339:61.

18. Sanchez-Madrid, F., A.M. Krensky, C.F. Ware, E. Robbins, J.L. Strominger, S.J. Burakoff, and T.A. Springer. 1982. Three distinct antigens associated with human T lymphocyte-mediated cytolysis: LFA-1, LFA-2, and LFA-3. *Proc. Natl. Acad. Sci. USA.* 79:7489.
19. Barnstable, C.J., W.F. Bodmer, G. Brown, G. Galfre, C. Milstein, A.F. Williams, and A. Ziegler. 1978. Production of monoclonal antibodies to group A erythrocytes, HLA and other human cell surface antigens: new tools for genetic analysis. *Cell.* 14:9.
20. Kearney, J.F., A. Radbruch, B. Liesegang, and K. Rajewsky. 1979. A new mouse myeloma cell line that has lost immunoglobulin expression but permits the construction of antibody-secreting hybrid cell lines. *J. Immunol.* 123:1548.
21. Julius, M.H., E. Simpson, and L.A. Herzenberg. 1973. A rapid method for the isolation of functional thymus-derived murine lymphocytes. *Eur. J. Immunol.* 3:645.
22. Timonen, T., C.W. Reynolds, J.R. Ortaldo, and R.B. Herberman. 1982. Isolation of human and rat natural killer cells. *J. Immunol. Methods.* 51:269.
23. Cantrell, D.A., and K.A. Smith. 1983. Transient expression of interleukin 2 receptors: consequences for T cell growth. *J. Exp. Med.* 158:1895.
24. Clarkson, S.B., and P.A. Ory. 1988. CD16 developmentally regulated IgG Fc receptors on cultured human monocytes. *J. Exp. Med.* 167:408.
25. Aruffo, A., and B. Seed. 1987. Molecular cloning of a CD28 cDNA by a high efficiency COS cell expression system. *Proc. Natl. Acad. Sci. USA.* 84:8573.
26. Gefter, M.L., D.H. Margulies, and M.D. Scharff. 1977. A simple method for polyethylene glycol-promoted hybridization of mouse myeloma cells. *Som. Cell Gen.* 3:231.
27. Cordell, J., B. Falini, O.N. Erber, A.K. Ghosh, Z. Abdulaziz, S. Macdonald, K. Polford, H. Stein, and D.Y. Mason. 1984. Immunoenzymatic labeling of monoclonal antibodies using immune complexes of alkaline phosphatase and monoclonal anti-alkaline phosphatase (APAAP complexes). *J. Histochem. Cytochem.* 31:219.
28. Kishimoto, T.K., K. O'Connor, and T.A. Springer. 1989. Leukocyte adhesion deficiency: Aberrant splicing of a conserved integrin sequence causes a moderate deficiency phenotype. *J. Biol. Chem.* 264:3588.
29. Laemmli, U.K. 1970. Cleavage of structural proteins during the assembly of the head of bacteriophage T4. *Nature (Lond.).* 227:680.
30. Dustin, M.L., and T.A. Springer. 1989. T cell receptor cross-linking transiently stimulates adhesiveness through LFA-1. *Nature (Lond.).* 341:619.
31. Dustin, M.L., J.G. Aguilar, M.L. Hibbs, R.S. Larson, S.A. Stacker, D.E. Staunton, A.J. Wardlaw, and T.A. Springer. 1989. Structure and regulation of the leukocyte adhesion receptor LFA-1 and its counter-receptors, ICAM-1 and ICAM-2. *Cold Spring Harbor Symp. Quant. Biol.* 54:753.
32. Rothlein, R., and T.A. Springer. 1986. The requirement for lymphocyte function-associated antigen 1 in homotypic leukocyte adhesion stimulated by phorbol ester. *J. Exp. Med.* 163:1132.
33. Tarentino, A., C. Gomez, and T. Plummer. 1985. Deglycosylation of asparagine-linked glycans by peptide:N-glycosidase F. *Biochemistry.* 24:4665.
34. Dustin, M.L., R. Rothlein, A.K. Bhan, C.A. Dinarello, and T.A. Springer. 1986. Induction by IL-1 and interferon, tissue distribution, biochemistry, and function of a natural adherence molecule (ICAM-1). *J. Immunol.* 137:245.
35. Boyd, A., I. Wicks, D. Wilkinson, J. Novotny, I. Campbell, S. Wawryk, L. Harrison, and G. Burns. 1989. Intercellular adhesion molecule 1 (ICAM-1): regulation and role in cell contact-mediated lymphocyte function. *In* Leucocyte Typing IV. W. Knapp, B. Dorken, W. Gilks, E. Rieber, R. Schmidt, H. Stein, and A. von dem Borne, editors. Oxford University Press, Oxford. pp. 684.
36. Pober, J.S., M.A. Gimbrone, Jr., L.A. Lapierre, D.L. Mendrick, W. Fiers, R. Rothlein, and T.A. Springer. 1986. Overlapping patterns of activation of human endothelial cells by interleukin 1, tumor necrosis factor and immune interferon. *J. Immunol.* 137:1893.
37. Wawryk, S.O., J.R. Novotny, I.P. Wicks, D. Wilkinson, D. Maher, E. Salvaris, K. Welch, J. Fecondo, and A.W. Boyd. 1989. The role of the LFA-1/ICAM-1 interaction in human leukocyte homing and adhesion. *Immunol. Rev.* 108:135.
38. Rice, G., J. Munro, and M. Bevilacqua. 1990. Inducible cell adhesion molecule 110 (INCAM-110) is an endothelial receptor for lymphocytes: A CD11/CD18-independent adhesion mechanism. *J. Exp. Med.* 171:1369.
39. Carlos, T., B. Schwartz, N. Kovach, E. Yee, M. Rosso, L. Osborn, G. Chi-Rosso, B. Newman, R. Lobb, and J. Harlan. 1990. Vascular cell adhesion molecule-1 (VCAM-1) mediates lymphocyte adherence to cytokine-activated cultured human endothelial cells. *Blood.* 76:965.
40. Schriever, F., A.S. Freedman, G. Freeman, E. Messner, G. Lee, J. Daley, and L.M. Nadler. 1989. Isolated human follicular dendritic cells display a unique antigenic phenotype. *J. Exp. Med.* 169:2043.
41. Johnson, J.P., B.G. Stade, B. Holzmann, W. Schwable, and G. Riethmuller. 1989. De novo expression of intercellular-adhesion molecule 1 in melanoma correlates with increased risk of metastasis. *Proc. Natl. Acad. Sci. USA.* 86:641.
42. Stade, B., G. Riethmuller, and J. Johnson. 1989. Potential role of ICAM-1 in metastasis formation in human malignant melanoma. *In* Leucocyte Typing IV. W. Knapp, B. Dorken, W. Gilks, E. Rieber, R. Schmidt, H. Stein, and A. von dem Borne, editors. Oxford University Press, Oxford. pp. 693.
43. Hamann, A., D.J. Westrich, A. Duijevstijn, E.C. Butcher, H. Baisch, R. Harder, and H.G. Thiele. 1988. Evidence for an accessory role of LFA-1 in lymphocyte-high endothelium interaction during homing. *J. Immunol.* 140:693.
44. Mackay, C.R., W.L. Marston, and L. Dudler. 1990. Naive and memory T cells show distinct pathways of lymphocyte recirculation. *J. Exp. Med.* 171:810.
45. Sanders, M.E, M.W. Makgoba, S.O. Sharrow, D. Stephany, T.A. Springer, H.A. Young, and S. Shaw. 1988. Human memory T lymphocytes express increased levels of three cell adhesion molecules (LFA-3, CD3, LFA-1) and three other molecules (UCHL1, CDw29, and Pgp-1) and have enhanced gamma interferon production. *J. Immunol.* 140:1401.
46. Dransfield, I., A. Buckle, and N. Hogg. 1990. Early events of the immune response mediated by leukocyte integrins. *Immunol. Rev.* 114:29.
47. Makgoba, M.W., M.E. Sanders, and S. Shaw. 1989. The CD2–LFA-3 and LFA-1–ICAM pathways: relevance to T-cell recognition. *Immunol. Today.* 10:417.
48. Bagnasco, M., G. Pesce, C. Pronzato, and G. Canonica. 1990. Functional involvement of the LFA-1/ICAM-1 adhesion system in the autologous mixed lymphocyte reaction. *Cell Immunol.* 128:362.
49. Diamond, M.S., D.E. Staunton, A.R. de Fougerolles, S.A.

Stacker, J. Garcia-Aguilar, M.L. Hibbs, and T.A. Springer. 1990. ICAM-1 (CD54)-A counter-receptor for Mac-1 (CD11b/CD18). *J. Cell Biol.* 111:3129.

50. van Noesel, C., F. Miedema, M. Brouwer, M.A. deRie, L.A. Aarden, and R.A.W. Van Lier. 1988. Regulatory properties of LFA-1 alpha and beta chains in human T-lymphocyte activation. *Nature (Lond.).* 333:850.
51. van Seventer, G., Y. Shimizu, K. Horgan, and S. Shaw. 1990. The LFA-1 ligand ICAM-1 provides an important costimulatory signal for T cell receptor-mediated activation of resting T cells. *J. Immunol.* 144:4579.
52. Nortamo, P., R. Salcedo, T. Timonen, M. Patarroyo, and C.G. Gahmberg. 1991. A monoclonal antibody to the human leukocyte adhesion molecule intercellular adhesion molecule-2: Cellular distribution and molecular characterization of the antigen. *J. Immunol.* 146:2530.